ACS APPLIED MATERIALS & INTERFACES

Research Article

www.acsami.org

Universal Electrode Interface for Electrocatalytic Oxidation of Liquid Fuels

Hualing Liao,[†] Zhipeng Qiu,[†] Qijin Wan,*[,†] Zhijie Wang,[†] Yi Liu,[†] and Nianjun Yang*[,†,‡]

[†]School of Chemistry and Environmental Engineering, Wuhan Institute of Technology, Wuhan, Hubei 430073, China

[‡]Institute of Materials Engineering, University of Siegen, 57076 Siegen, Germany

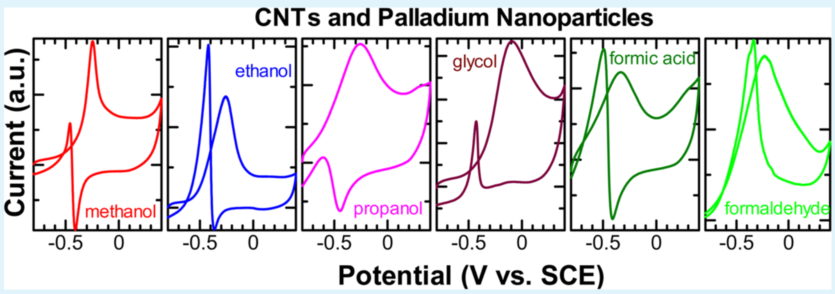

ABSTRACT: Electrocatalytic oxidations of liquid fuels from alcohols, carboxylic acids, and aldehydes were realized on a universal electrode interface. Such an interface was fabricated using carbon nanotubes (CNTs) as the catalyst support and palladium nanoparticles (Pd NPs) as the electrocatalysts. The Pd NPs/CNTs nanocomposite was synthesized using the ethylene glycol reduction method. It was characterized using transmission electron microscopy, energy dispersive X-ray spectroscopy, X-ray diffraction, voltammetry, and impedance. On the Pd NPs/CNTs nanocomposite coated electrode, the oxidations of those liquid fuels occur similarly in two steps: the oxidations of freshly chemisorbed species in the forward (positive-potential) scan and then, in the reverse scan (negative-potential), the oxidations of the incompletely oxidized carbonaceous species formed during the forward scan. The oxidation charges were adopted to study their oxidation mechanisms and oxidation efficiencies. The oxidation efficiency follows the order of aldehyde (formaldehyde) > carboxylic acid (formic acid) > alcohols (ethanol > methanol > glycol > propanol). Such a Pd NPs/CNTs nanocomposite coated electrode is thus promising to be applied as the anode for the facilitation of direct fuel cells.

KEYWORDS: *electrocatalytic oxidation, liquid fuels, carbon nanotubes, palladium nanoparticles, reaction mechanism, oxidation efficiency, fuel cells*

INTRODUCTION

Fuel cells are excellent power sources due to their high energy densities, low pollutant emission, and easy handling.[1−4] Direct alcohol fuel cells (DAFCs) have shown more advantages over polymer electrolyte fuel cells (PEFC), such as high volumetric energy densities of alcohols and easier storage and transport of alcohols compared to hydrogen.[1] Numerous alcohols including methanol, ethanol, ethylene glycol, and glycerol have been thus used as the fuels for DAFCs. However, the oxidation rates of alcohols were too slow, and thus, the electrocatalysts for the oxidation of alcohols are highly required. During the past decades, many achievements and progress have been made regarding the synthesis of the electrocatalysts and their applications for the electrocatalytic oxidation of alcohols.[4−34] Metal platinum based catalysts (bulk or nanoparticles) play the main role and have been extensively utilized.[1−8] They showed good catalytic performance toward the oxidation of most alcohols. However, they are extremely expensive and have limited resources. Moreover, carboxyl species (mainly carbon oxide), the products from the oxidation of alcohols, adsorb strongly on the electrode surface. The surface of the catalysts is then poisoned, resulting in the reduction and eventually the loss of the catalytic ability of the Pt based electrocatalysts.

To solve these problems for the electrocatalytic oxidation of alcohols, novel metal electrocatalysts (e.g., palladium, nickel, zinc, gold, ruthenium, etc.) have been tested.[1,5−23] In most cases, the electrocatalysts are deposited chemically or electrochemically on the nanostructured catalyst supports. These smart electrocatalytic architectures/nanocomposites exhibit higher efficiencies for oxidation of alcohols. Moreover they are more cost-effective than platinum based catalytic systems. The poisoning effect has been reduced as well.[9−23] As for the catalyst support, the carbon nanotube (CNT) is one of the mostly utilized supports.[1,24−37] This is because CNT has a large surface area and high electrical and thermal conductivity, as well as long-term stability. On the other hand, it is known that in an alkaline environment palladium nanoparticles (Pd NPs) are highly active for the oxidation of a large variety of substances.[1,22−33] CNTs loaded with palladium nanoparticles,

Received: July 25, 2014
Accepted: September 29, 2014
Published: September 29, 2014

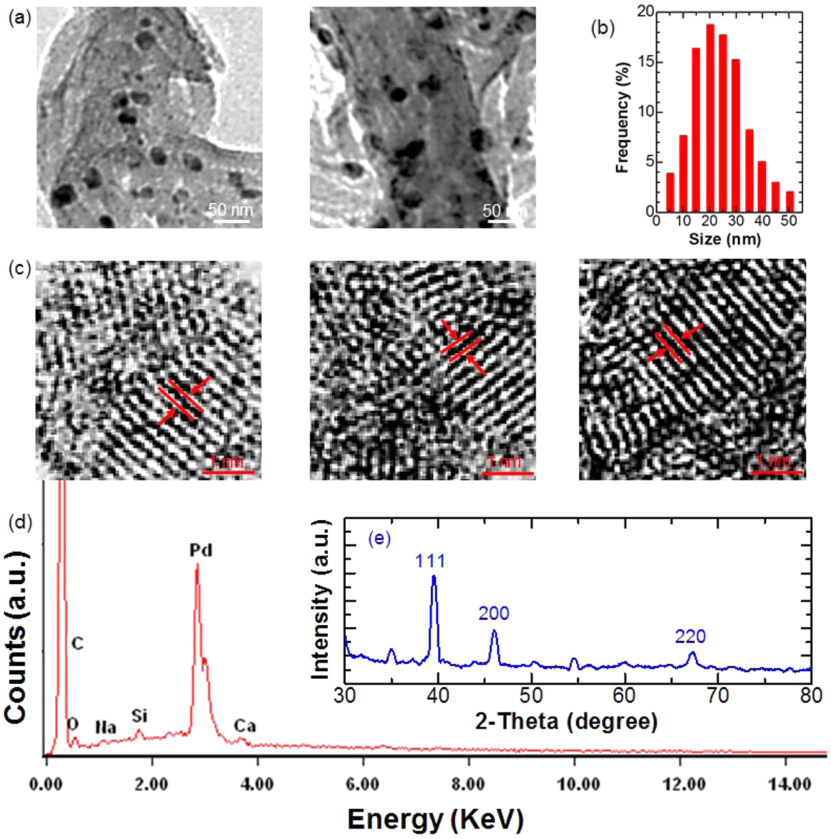

Figure 1. Characterization of the Pd NPs/CNTs nanocomposite: TEM images (a, c), EDX spectrum (d), and XRD patterns (e) of CNTs loaded with Pd NPs; (b) size histogram of Pd NPs. The bars and arrows in (c) are for eye-guidance to show the interplanar spacing of Pd NPs.

namely, the Pd NPs/CNTs nanocomposite, thus have been applied to achieve rapid and efficient oxidization of different liquid fuels.[24−37] Numerous approaches have been developed to produce Pd NPs/CNTs nanocomposites. Those nanocomposites have been applied successfully to achieve electrocatalytic oxidation of one or two liquid fuels. In most cases, the electrocatalytic oxidation peak currents were adopted to analyze the suitability, efficiency, and possibility of those systems for fuel cell applications. Actually, relatively few reports concentrated on the detailed investigation as well as the comparison of the reaction mechanisms and the efficiencies of the electrocatalytic oxidation of different types of liquid fuels (e.g., alcohols, aldehydes, and carboxylic acids) on such a Pd NPs/CNTs nanocomposite.

The aim of this work is to investigate electrocatalytic oxidations of more than two kinds of liquid fuels on the Pd NPs/CNTs nanocomposite coated electrode, to study and compare the oxidation mechanisms and efficiencies of liquid fuels on this electrode, as well as to develop new technique to analyze the oxidation mechanisms and efficiencies of liquid fuels. Herein, we investigated in alkaline media the electrocatalytic oxidation reactions of three types (alcohols, aldehydes, and carboxylic acids) of six liquid fuels (methanol, ethanol, propanol, glycol, formic acid, and formaldehyde) on a Pd NPs/CNTs nanocomposite. The ethylene glycol reduction method was used to prepare Pd NPs/CNTs nanocomposites. Such Pd NPs/CNTs nanocomposites were characterized with transmission electron microscopy (TEM), energy dispersive X-ray spectroscopy (EDX), X-ray diffraction (XRD), and electrochemical techniques (voltammetry and impedance). Direct casting of Pd NPs/CNTs nanocomposites on a glassy carbon electrode led to the fabrication of a Pd NPs/CNTs nanocomposite coated electrode. Instead of adopting the electrocatalytic oxidation peak current, we utilized for the first time the oxidation charge in the forward scan as well as that in the reverse scan as the parameter to study the electrocatalytic oxidation mechanisms and efficiencies of different liquid fuels on the Pd NPs/CNTs nanocomposite coated electrode. The experimental conditions affecting their oxidation mechanisms and efficiencies were discussed, including the concentration of alkaline solutions, the concentration of liquid fuels, and the amount of Pd NPs and CNTs in the nanocomposite. The stability of the Pd NPs/CNTs nanocomposite coated electrode for those electrocatalytic oxidation reactions was tested as well.

■ RESULTS AND DISCUSSION

Figure 1a shows two typical TEM images of CNTs loaded with Pd NPs where numerous nanoparticles are clearly seen. These spherical nanoparticles are relatively homogeneously dispersed. Some agglomerations are seen as well. The size histogram of the nanoparticles was measured from 100 random particles in an arbitrarily chosen area. As shown in Figure 1b, it reveals a size distribution in the range of 5−50 nm. Most of them (∼65%) are in the size of 15−30 nm. The high resolution TEM images in Figure 1c show the same type of lattice fringe of nanoparticles. As indicated with bars and arrows, the interplanar spacing is about 0.24 nm, indicating Pd(111) planes. The energy dispersive X-ray (EDX) spectrum of CNTs loaded with Pd NPs (Figure 1d) shows a sharp peak at about 2.9 keV, confirming the existence of Pd NPs on CNTs. Other diffraction peaks are from the materials during the sample preparation process. Furthermore, the XRD patterns of such a nanocomposite shown in Figure 1e display typical face-centered cubic (fcc) patterns. The peaks at 39.5°, 46.1°, and 67.3° are assigned to the Pd (111), (200), and (220), respectively. Therefore, Pd NPs have been loaded on CNTs.

Such a nanocomposite was then applied for the construction of the Pd NPs/CNTs nanocomposite coated electrode. The nanocomposite was dispersed and dried on a glassy carbon electrode to form a Pd NPs/CNTs nanocomposite coated electrode. Electrochemical techniques were applied to investigate electrochemical redox activity of the Pd NPs/CNTs nanocomposite coated electrode. The redox couple of $Fe(CN)_6^{3-/4-}$ was utilized as the probe. Figure 2 shows the Nyquist plots recorded at open circuit potentials on a bare glassy carbon electrode (a), the CNTs coated electrode (b), and the Pd NPs/CNTs nanocomposite coated electrode (c). The frequency range was varied from 100 kHz to 0.01 Hz. A big semicircle (about 350 Ω) at the high frequency domain and a straight line at the low frequency region appears in the Nyquist plot for a bare glassy carbon electrode (Figure 2a). On the CNTs coated electrode (b), the diameter of the semicircle reduces to 60 Ω at high frequency range. While for the Pd NPs/CNTs nanocomposite coated electrode (c), only a straight line is obtained. Since the diameter of the semicircle in the Nyquist plot is directly related with the electron transfer resistance of the electrode, these results prove that the electron transfer rate on the Pd NPs/CNTs nanocomposite coated electrode is the fastest. This was further confirmed with the voltammetric behavior of $Fe(CN)_6^{3-/4-}$ on those electrodes. The highest peak current and the smallest peak difference (about 62 mV) for the redox reaction of $Fe(CN)_6^{3-/4-}$ were achieved on the Pd NPs/CNTs nanocomposite coated electrode. Due to enhanced ion transport and ready charge transfer on such an electrode, it is possible to enhance slow rates of electrode reactions (e.g., the oxidation of alcohols).

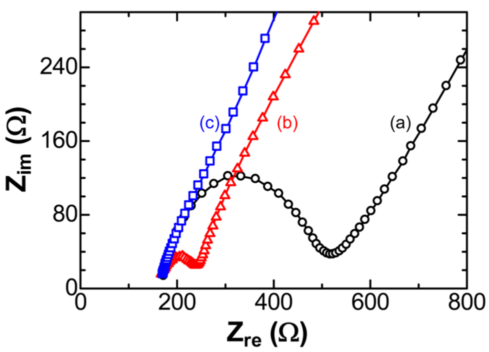

Figure 2. Electrochemical characterization of the Pd NPs/CNTs nanocomposite coated electrode: Nyquist plots of 5.0 mM $Fe(CN)_6^{3-/4-}$ in 0.1 M KCl on a bare glassy carbon electrode (a), the CNTs coated electrode (b), and the Pd NPs/CNTs nanocomposite coated electrode (c). The spectra were recorded at open circuit potentials.

Electrochemical oxidations of six liquid fuels (methanol, ethanol, propanol, glycol, formic acid, and formaldehyde) were then conducted on the Pd NPs/CNTs nanocomposite coated electrode, respectively. Figure 3 compares first the voltammetric behavior of methanol on a glassy carbon electrode (Figure 3a), the CNTs coated electrode (Figure 3b), and the Pd NPs/CNTs nanocomposite coated electrode (Figure 3c). On a bare glassy carbon electrode and on the CNTs coated electrode, only capacitive currents are recorded, indicating that no oxidation of methanol occurs. The capacitive current of the CNTs coated electrode is bigger than that of a glassy carbon electrode. This is due to the enlarged active area of the electrode as well as the change of the normalized capacitance of the electrode materials. On the Pd NPs/CNTs nanocomposite coated electrode, double and crossed anodic waves are noticed. One sharp oxidation peak is located at −0.24 V with a peak current of 1.76 μA; another oxidation peak has a peak potential of −0.46 V and a peak current of 0.59 μA. When methanol is replaced with ethanol, a similar-shaped voltammogram is obtained (Figure 3d). Namely, double and crossed anodic waves are seen as well. The peak potential and current of the broad anodic wave are −0.26 V and 1.23 μA, respectively. For the sharp peak, they are −0.42 V and 1.80 μA, respectively. Therefore, in alkaline electrolytes, the oxidation rates of alcohols have been significantly improved on the Pd NPs/CNTs nanocomposite coated electrode. The peak potentials for the oxidation of methanol and ethanol on the Pd NPs/CNTs nanocomposite coated electrode are slightly negative (about 10−20 mV) compared to those obtained on the electrode only coated with Pd NPs (the Pd NPs coated electrode), as shown in the cyclic voltammograms for the oxidation of methanol in Figure 3e and for the oxidation of ethanol in Figure 3f. This result confirms the key role of Pd NPs in those electrocatalytic oxidation reactions. The oxidation peak currents on the Pd NPs/CNTs nanocomposite coated electrode are about 2−5 times higher than those on the Pd NPs coated electrode, indicating more active/adsorption sites of the Pd NPs/CNTs nanocomposite electrode for the oxidation of those alcohols. Subsequently the Pd NPs/CNTs nanocomposite coated electrode is the best for the electrocatalytic oxidation of alcohols.

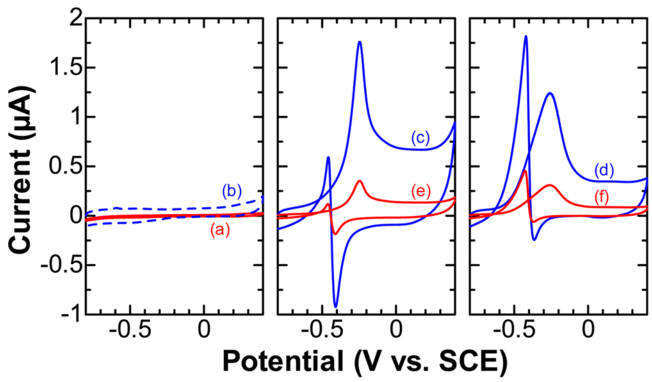

Figure 3. Electrocatalytic oxidations of alcohols: cyclic voltammograms of 5.0 mM methanol (a, b, c, e) and ethanol (d, f) on a bare glassy carbon electrode (a), the CNTs coated electrode (b), the Pd NPs/CNTs nanocomposite coated electrode (c, d), and the Pd NPs coated electrode (e, f). The supporting electrolyte was 2.0 M KOH. The scan rate was 100 mV s^{-1}.

For electrocatalytic oxidation of methanol and related alcohols, it is widely accepted[38−44] that the oxidation wave in the forward scan is due to the oxidation of freshly chemisorbed species derived from alcohol or alcohol adsorption, while the second one in the reverse scan is primarily ascribed to the removal of the incompletely oxidized carbonaceous species formed during the forward scan. The ratio of the peak current in the forward scan ($I_{p,f}$) to the one in the reverse scan ($I_{p,r}$) has been proposed to describe the catalyst tolerance to the carbonaceous species on the electrode surface. A higher $I_{p,f}/I_{p,r}$ ratio suggests a higher removal efficiency of the poisoning species from the electrode surface. In our case, on the Pd NPs/CNTs nanocomposite coated electrode, the $I_{p,f}/I_{p,r}$ ratios were estimated to be 2.98 and 0.68 for the oxidation of methanol and ethanol, respectively. Therefore, the removal of poisoning species is faster and more efficient for methanol than that for ethanol. Through integrating anodic waves, the individual charges for the oxidation waves in the forward scan and in the reverse scan were further estimated on the Pd NPs/CNTs nanocomposite coated electrode. The oxidation charges in the forward scan (Q_f) for methanol and ethanol were 3.9 and 4.0 μC, respectively. These values suggest that a quite similar amount of methanol and ethanol have been oxidized in the forward scan on the Pd NPs/CNTs nanocomposite coated electrode. In the reverse scan, the oxidation charges (Q_r) were 0.2 μC for methanol and 1.1 μC for ethanol, respectively. In other words, more poisoning species from the oxidation of ethanol are adsorbed on the electrode surface than those from the oxidation of methanol. The difference of Q_r (0.9 μC) for methanol from that for ethanol results probably from the oxidation of some amount of freshly chemisorbed ethanol in the reverse scan on the Pd NPs/CNTs nanocomposite coated electrode.

To get more details about the adsorption of alcohols as well as the mechanisms of the oxidation of alcohols on the Pd NPs/CNTs nanocomposite coated electrode, we investigated the variation of the oxidation changes in the forward scan (Q_f) and in the reverse scan (Q_r) as a function of the concentration of alkaline solutions (C_{KOH}) and the concentration of alcohols (C_{ROH}). Figure 4 shows those results. As shown in Figure 4a, an

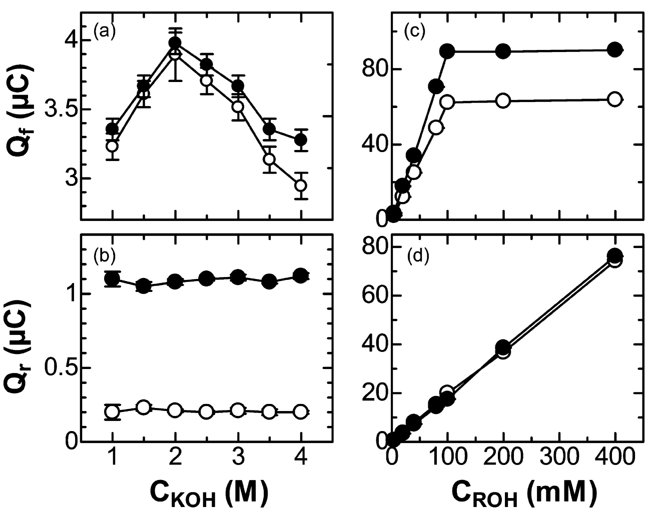

Figure 4. Reaction mechanism of electrocatalytic oxidations of alcohols on the Pd NPs/CNTs nanocomposite coated electrode: the charge in the forward scan (Q_f) and in the reverse scan (Q_r) for the oxidation of methanol (open dots) and ethanol (solid dots) as a function of the concentration of KOH (C_{KOH}) (a, b) and the concentration of alcohol (C_{ROH}) (c, d). Some error bars in (b), (c), and (d) are not visible due to the scales.

increase of C_{KOH} up to 2.0 M leads to the enhancement of Q_f for both methanol and ethanol. A further increase of C_{KOH} on the contrary reduces Q_f. Differently from Q_f, Q_r for both methanol and ethanol does not vary as a function of C_{KOH} (Figure 4b). On the other hand, Q_r reaches a maximum value at C_{ROH} = 100 mM and then stays almost constant (Figure 4c), while Q_r increases linearly with C_{ROH} for methanol and ethanol in a range of 4 to 400 mM (Figure 4d). Assuming that OH^- adsorption on the surface of Pd NPs is independent of C_{ROH}, the rate-limiting step of the electrocatalytic oxidation of alcohols on the Pd NPs/CNTs nanocomposite coated electrode involves the following reactions:[41−44]

$$Pd + OH^- \leftrightarrow Pd\text{-}(OH)_{ads} + e^- \quad (1)$$

$$Pd + RCOH \leftrightarrow Pd\text{-}(RCOH)_{ads} \quad (2)$$

$$Pd\text{-}(RCOH)_{ads} + 3OH^- \rightarrow Pd\text{-}(RCO)_{ads} + 3H_2O + 3e^- \quad (3)$$

To optimize the Pd NPs/CNTs nanocomposite coated electrode and to inspect further its catalytic efficiency toward the electrocatalytic oxidations of alcohols, we plotted out in Figure 5 the dependence of the total oxidation charge, Q (= Q_f

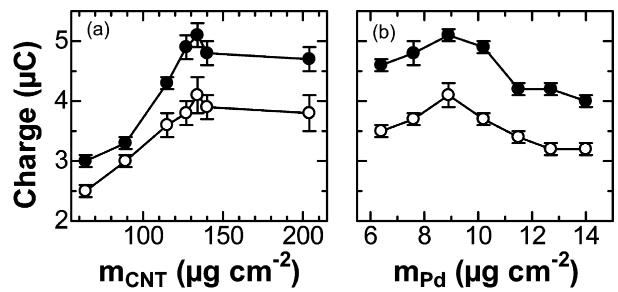

Figure 5. Optimization of the Pd NPs/CNTs nanocomposite coated electrode: the charges for the oxidation of methanol (open dots) and ethanol (solid dots) as a function of the amount of CNTs used (m_{CNT}) (a) and the amount of Pd NPs (m_{Pd}) (b).

+ Q_r) for methanol (open dots) and ethanol (solid dots) on the amount of CNTs (m_{CNT}) and the amount of Pd NPs (m_{Pd}) used in the Pd NPs/CNTs nanocomposite. m_{CNT} and m_{Pd} were normalized with the electrode area of a bare glassy carbon electrode. The variation of m_{CNT} and m_{Pd} was realized by varying the concentration (0.2 to 4.0 mg mL^{-1}) and the volume (0.5 to 10 μL) of the suspension of Pd NPs/CNTs nanocomposite. The values of Q for ethanol are generally higher than those for methanol. When both m_{CNT} and m_{Pd} increase, the Qs for methanol and ethanol are enhanced. When m_{CNT} = 134 μg cm^{-2} and m_{Pd} = 89.0 μg cm^{-2} were applied, the maximum Q for both methanol and ethanol were realized. A further increase in either m_{CNT} or m_{Pd} leads to a reduction of Qs. Assuming the Pd NPs distribute homogeneously on CNTs, the ratio of palladium atoms to carbon atoms in such a nanocomposite is 1:13. Taking the densities of palladium bulk (12.0 g cm^{-3}) and carbon (1.8 g cm^{-3}) into account, the optimized loading ratio of Pd NPs on CNTs is 51%. The nanocomposite with 134 μg cm^{-2} CNTs and 89.0 μg cm^{-2} Pd NPs was applied further for the electrocatalytic oxidation of other liquid fuels.

Electrocatalytic oxidations of other alcohols (propanol and glycol), carboxylic acid (formic acid), and aldehyde (formaldehyde) were then tested on the Pd NPs/CNTs nanocomposite coated electrode. As shown in Figure 6, the shapes of the voltammograms are similar to those for the oxidation of methanol and ethanol, while the scales of the oxidation currents are different. The peak potential for the oxidation of propanol is located at −0.35 V in the forward scan, and in the reverse scan, it is at −0.61 V (Figure 6a). The ratio of $(I_{p,f}/I_{p,r})_{propanol}$ and $Q_{propanol}$ (= Q_f + Q_r) were estimated to be 15 and 0.95 μC, respectively. For glycol (Figure 6b), the peak potential in the

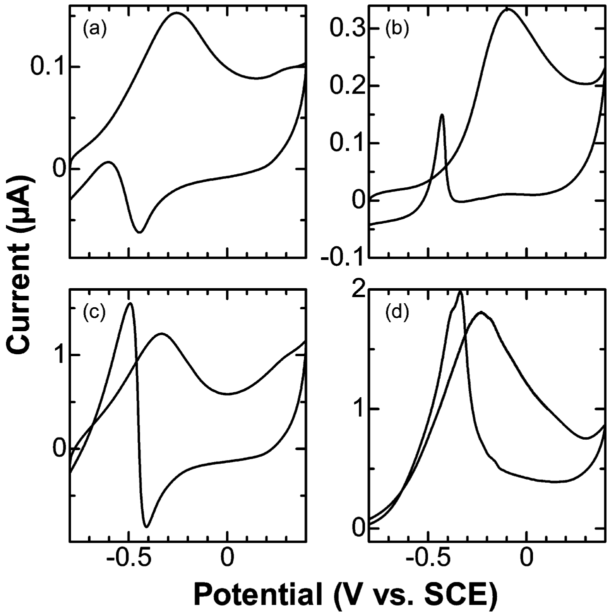

Figure 6. Electrocatalytic oxidations of different liquid fuels on the Pd NPs/CNTs nanocomposite coated electrode: cyclic voltammograms of 5.0 mM (a) propanol, (b) glycol, (c) formic acid, and (d) formaldehyde in 2.0 M KOH at a scan rate of 100 mV s^{-1}.

forward scan shifts to −0.1 V and the one in the reverse scan to −0.61 V. The ratio of $(I_{p,f}/I_{p,r})_{glycol}$ and Q_{glycol} are 2.5 and 2.6 μC, respectively. For formic acid (Figure 6c), an oxidation wave at −0.33 V in the forward scan and a sharp oxidation at −0.50 V in the reverse scan are seen, corresponding to two parallel reaction pathways, namely, direct and indirect ways.[45−49] The wave in the forward scan is due to the direct oxidation of formic acid to form carbon dioxide.[45−49] While the wave in the reverse scan is related to the oxidation of the intermediate carbon monooxide generated from the dissociative adsorption step.[50−54] The ratio of $(I_{p,f}/I_{p,r})_{formic\ acid}$ and $Q_{formic\ acid}$ were estimated to be 0.87 and 9.6 μC, respectively. These demonstrate that the electrocatalytic oxidation of formic acid on the Pd NPs/CNTs nanocomposite coated electrode proceeds mainly through the direct pathway. The peak potentials for the oxidation of formaldehyde (Figure 6d) are at −0.24 V in the forward scan and at −0.34 V in the reverse scan. The oxidation current in the forward scan is due to the oxidation of formaldehyde into formic acid, which is further oxidized into carbon di/mono-oxide, contributing to the oxidation current in the reverse scan.[55−58] The ratio of $(I_{p,f}/I_{p,r})_{formaldehyde}$ and $Q_{formaldehyde}$ were estimated to be 0.93 and 18.4 μC, respectively. Control experiments show that no oxidation of those four liquid fuels was realized on either a bare glassy carbon electrode or the CNTs coated electrode. Therefore, the Pd NPs/CNTs nanocomposite coated electrode can be applied for the electrocatalytic oxidations of different liquid fuels.

The long-term activity and durability of the Pd NPs/CNTs nanocomposite coated electrode toward the electrocatalytic oxidations of six liquid fuels were assessed. Figure 7 shows the current−time curves for methanol (a), ethanol (b), propanol (c), glycol (d), formic acid (e), and formaldehyde (f). A constant potential of 0 V (vs SCE) was applied. This potential was selected from the voltammograms shown in Figures 3 and 6. The highest initial and the limiting oxidation currents are from the electrocatalytic oxidation of formaldehyde (Figure 7f).

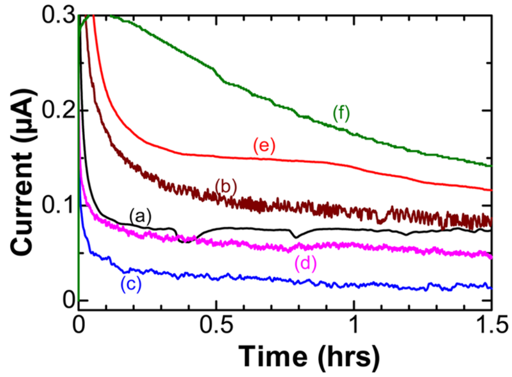

Figure 7. Stability and durability of the Pd NPs/CNTs nanocomposite coated electrode toward the electrocatalytic oxidations of liquid fuels: Current−time curves at a constant potential of 0 V vs SCE for electrocatalytic oxidations of 0.5 mM methanol (a), ethanol (b), propanol (c), glycol (d), formic acid (e), and formaldehyde (f) in 2.0 M KOH.

The lowest oxidation currents are seen for the oxidation of propanol (Figure 7c). Their oxidation currents on the Pd NPs/CNTs nanocomposite coated electrode follow the order of formaldehyde (Figure 7f), formic acid (Figure 7e), ethanol (Figure 7b), methanol (Figure 7a), glycol (Figure 7d), and propanol (Figure 7c). In other words, the Pd NPs/CNTs nanocomposite coated electrode has the highest catalytic performance for formaldehyde. Moreover, the Pd NPs/CNTs nanocomposite coated electrode shows long superior activity and durability toward the oxidations of those liquid fuels, judging from the reaction time (within 1.5 h), the initial current, and the limiting current. Combining the results from cyclic voltammetry with those in Figure 7, one can conclude that on the Pd NPs/CNTs nanocomposite coated electrode the oxidation efficiency follows the order of aldehyde (formaldehyde) > carboxylic acid (formic acid) > alcohols (ethanol > methanol > glycol > propanol).

CONCLUSION

In summary, a universal electrode has been constructed using palladium nanoparticles as the electrocatalysts and carbon nanotubes as the catalyst support. On such a nanocomposite coated electrode, the electrocatalytic oxidations of three types (alcohols, carboxylic acids, and aldehydes) of six liquid fuels (methanol, ethanol, propanol, glycol, formic acid, and formaldehyde) have been achieved. The oxidations of those liquid fuels occur similarly in two steps: the oxidation of freshly chemisorbed species in the forward (positive-potential) scan and then; in the reverse scan (negative-potential), the oxidation of the incompletely oxidized carbonaceous species formed during the forward scan. Using the oxidation charges in the forward and in the reverse scan separately and totally, the oxidation efficiency was found in the order of aldehyde (formaldehyde) > carboxylic acid (formic acid) > alcohols (ethanol > methanol > glycol > propanol). Additionally, this electrode shows long durability toward the oxidations of those liquid fuels. It is thus promising to be adopted as the anode for direct alcohol fuel cell applications.

EXPERIMENTAL SECTION

Multiwalled carbon nanotubes (CNTs, purity >95%; concentration of amorphous carbon <3%; the concentration of catalyst residue <0.2%; special surface area, 40−300 $m^2\ g^{-1}$; thermal conductivity, ∼2000 W

m^{-1} K^{-1}) were bought from Shenzhen Nanotech LTD (Shenzhen, China). All chemicals were purchased from Shanghai Chemical Reagent Co. LTD (Shanghai, China) and were analytical grade reagents. TEM images of CNTs loaded with Pd NPs were recorded on a 200 kV high-resolution transmission electron microscope (HRTEM, JEOL-2000). The X-ray diffraction (XRD) spectra were recorded with a Bruke D8 diffractometer (Hannover, Germany). A Cu Kα radiation (40 kV, 40 mA) was used with a Ni filter. Electrochemical experiments were conducted at room temperature (25 °C) on a CHI760B electrochemical workstation (Chenhua Instrument Company, Shanghai, China) with a standard three-electrode configuration. Either a bare or a modified glassy carbon electrode (e.g., the CNTs coated electrode, the Pd NPs/CNTs nanocomposite coated electrode, and the Pd NPs coated electrode) acted as the working electrode, a platinum foil as the counter electrode, and a saturated calomel electrode (SCE) as the reference electrode. The Pd NPs/CNTs nanocomposite coated electrode was fabricated by directly casting ink-like suspension, namely, the Pd NPs/CNTs nanocomposite, on a clean glassy carbon electrode surface. The volume of the suspension was varied from 0.5 to 10 μL, and the concentration of the suspension was changed from 0.2 to 4.0 mg mL^{-1}. After drying the electrode under a UV-lamp in air, the Pd NPs/CNTs nanocomposite coated electrode was formed. To obtain a clean electrode, the glassy carbon electrode with a geometric area of 0.0785 cm^2 was first polished using alumina slurries and then cleaned with ethanol and water.

Prior to preparation of the ink-like (the Pd NPs/CNTs nanocomposite) suspension, CNTs were pretreated in the same way as reported.[59,60] Briefly, 500 mg of CNTs was oxidized at 400 °C for 30 min to remove amorphous carbon particles. The oxidized CNTs were then dispersed in 60 mL of 6.0 M HCl for 4 h in an ultrasonic bath to eliminate metal oxide catalysts. They were further washed with water sufficiently (until the pH of the washing solution was close to 7.0) and dried in air at room temperature. The purified CNTs were then oxidized in a mixture of concentrated sulfuric and nitric acid (v/v = 3:1) at 50−60 °C in an ultrasonication for 6 h. The resultant solution was filtered through a poly(tetra Xuoroethylene) membrane with a 200 nm pore size. The solid powders were washed thoroughly with water to remove any residual acid and then dried at 60 °C for 2 h. They were used for loading Pd NPs.

Loading of Pd NPs onto CNTs was achieved using a reduction method in an ethylene glycol solution[61,62] Sodium citrate (50 mM) and palladium chloride (25 mM) solutions were used. The loading of Pd NPs on CNTs was conducted via dispersing treated CNTs (0.05 g) in the suspension of Pd NPs. Ultrasonication and stirring were applied. The pH value of ethylene glycol solution was adjusted to 9.0 by dropwise addition of a 1.0 M KOH solution. After refluxing this suspension at 160 °C in an oil bath for 6 h, the resulting material was centrifuged and the slurry was obtained. Washing this slurry with deionized water and ethanol, followed by drying at 80 °C, led to the production of Pd NPs loaded CNTs. This material (3.0 mg) was then dispersed homogeneously in 1.0 mL of isopropyl alcohol by sonication for 30 min. Such an ink-like suspension was applied to coat a clean glassy electrode.

■ AUTHOR INFORMATION

Corresponding Authors

*E-mail: qijinwan@mail.wit.edu.cn.

*E-mail: nianjun.yang@uni-siegen.de.

Notes

The authors declare no competing financial interest.

■ ACKNOWLEDGMENTS

The authors are thankul for the financial support from the National Natural Science Foundation of China (21275113 and 21075096).

■ REFERENCES

(1) Bianchini, C.; Shen, P. K. Palladium-Based Electrocatalysts for Alcohol Oxidation in Half Cells and in Direct Alcohol Fuel Cells. *Chem. Rev.* **2009**, *109*, 4183−4206.

(2) Moghaddam, R. B.; Peter, P. G. Support Effects on the Oxidation of Methanol at Platinum Nanoparticles. *Electrochem. Commun.* **2011**, *13*, 704−706.

(3) Moghaddam, R. B.; Peter, P. G. Support Effects on the Oxidation of Ethanol at Pt Nanoparticles. *Electrochim. Acta* **2012**, *65*, 210−215.

(4) Wietecha, M. S.; Zhu, J.; Gao, G. H.; Wang, N.; Feng, H.; Gorring, M. L.; Kasner, M. L.; Hou, S. F. Platinum Nanoparticles Anchored on Chelating Group-Modified Graphene for Methanol Oxidation. *J. Power Sources* **2012**, *198*, 30−35.

(5) Tominaka, S.; Momma, T.; Osaka, T. Electrodeposited Pd-Co Catalyst for Direct Methanol Fuel Cell Electrodes: Preparation and Characterization. *Electrochim. Acta* **2008**, *53*, 4679−4686.

(6) Hudiono, Y.; Choi, S.; Shu, S.; Koros, W. J.; Tsapatsis, M.; Nair, S. Porous Layered Oxide/Nafion Nanocomposite Membranes for Direct Methanol Fuel Cell Applications. *Microporous Mesoporous Mater.* **2009**, *118*, 427−434.

(7) Wee, J. H. Which Type of Fuel Cell Is More Competitive for Portable Application: Direct Methanol Fuel Cells or Direct Borohydride Fuel Cells? *J. Power Sources* **2006**, *161*, 1−10.

(8) Shen, P. K.; Xu, C. W. Alcohol Oxidation on Nanocrystalline Oxide Pd/C Promoted Electrocatalysts. *Electrochem. Commun.* **2006**, *8*, 184−188.

(9) Chen, L. C.; Yu, T. L.; Lin, H. L.; Yeh, S. H. Nafion/PTFE and Zirconium Phosphate Modified Nafion/PTFE Composite Membranes for Direct Methanol Fuel Cells. *J. Membr. Sci.* **2008**, *307*, 10−20.

(10) Cao, D. X.; Bergens, S. H. Pt−Ru_{adatom} Nanoparticles as Anode Catalysts for Direct Methanol Fuel Cells. *J. Power Sources* **2004**, *134*, 170−180.

(11) Lamy, C.; Rousseau, S.; Belgsir, E. M.; Coutanceau, C.; Leger, J. M. Recent Progress in the Direct Ethanol Fuel Cell: Development of New Platinum-Tin Electrocatalysts. *Electrochim. Acta* **2004**, *49*, 3901−3908.

(12) Vigier, F.; Coutanceau, C.; Perrard, A.; Belgsir, E. M.; Lmay, C. Development of Anode Catalysts for a Direct Ethanol Fuel Cell. *J. Appl. Electrochem.* **2004**, *34*, 439−446.

(13) Dimos, M. M.; Blanchard, G. J. Evaluating the Role of Pt and Pd Catalyst Morphology on Electrocatalytic Methanol and Ethanol Oxidation. *J. Phys. Chem. C* **2010**, *114*, 6019−6026.

(14) Cui, X. Z.; Guo, L. M.; Cui, F. M.; He, Q. J.; Shi, J. L. Electrocatalytic Activity and CO Tolerance Properties of Mesostructured Pt/WO_3 Composite as an Anode Catalyst for PEMFCs. *J. Phys. Chem. C* **2009**, *113*, 4134−4138.

(15) Kim, S.; Sohn, H. J.; Park, S. J. Preparation and Characterization of Carbon-Related Materials Supports for Catalysts of Direct Methanol Fuel Cells. *Curr. Appl. Phys.* **2010**, *10*, 1142−1147.

(16) Hull, R. V.; Li, L.; Xing, Y. C.; Chusuei, C. C. Pt Nanoparticle Binding on Functionalized Multiwalled Carbon Nanotubes. *Chem. Mater.* **2006**, *18*, 1780−1788.

(17) Takeguchi, T.; Anzai, Y.; Kikuchi, R.; Eguchi, K.; Ueda, W. Preparation and Characterization of CO-Tolerant Pt and Pd Anodes Modified with SnO_2 Nanoparticles for PEFC. *J. Electrochem. Soc.* **2007**, *154*, B1132−B1137.

(18) Lu, G. Q.; Chrzanowski, W.; Wieckowski, A. Catalytic Methanol Decomposition Pathways on a Platinum Electrode. *J. Phys. Chem. B* **2000**, *104*, 5566−5572.

(19) Jusys, Z.; Behm, R. J. Methanol Oxidation on a Carbon-Supported Pt Fuel Cell Catalyst - A Kinetic and Mechanistic Study by Differential Electrochemical Mass Spectrometry. *J. Phys. Chem. B* **2001**, *105*, 10874−10883.

(20) Wen, Y.; Ye, J. S.; Zhang, W. D.; Sheu, F. S.; Xu, G. Q. Electrocatalytic Oxidation of Methanol on a Platinum Modified Carbon Nanotube Electrode. *Microchim. Acta* **2008**, *162*, 235−242.

(21) Yen, C. H.; Shimizu, K.; Lin, Y. Y.; Bailey, F.; Cheng, L. F.; Wai, C. M. Chemical Fluid Deposition of Pt-Based Bimetallic Nanoparticles

on Multiwalled Carbon Nanotubes for Direct Methanol Fuel Cell Application. *Energy Fuels* **2007**, *21*, 2268−2271.

(22) Koenigsmann, C.; Semple, D. B.; Sutter, E.; Tobierre, S. E.; Wong, S. S. Ambient Synthesis of High-Quality Ruthenium Nanowires and the Morphology-Dependent Electrocatalytic Performance of Platinum-Decorated Ruthenium Nanowires and Nanoparticles in the Methanol Oxidation Reaction. *ACS Appl. Mater. Interfaces* **2013**, *5*, 5518−5530.

(23) Patra, S.; Viswanath, B.; Barai, K.; Ravishankar, N.; Munichandraiah, N. High-Surface Step Density on Dendritic Pd Leads to Exceptional Catalytic Activity for Formic Acid Oxidation. *ACS Appl. Mater. Interfaces* **2010**, *2*, 2965−2969.

(24) Ren, L.; Yang, L.; Yu, P.; Wang, Y.; Mao, L. Electrochemical Post-Treatment of Infinite Coordination Polymers: An Effective Route to Preparation of Pd Nanoparticles Supported onto Carbon Nanotubes with Enhanced Electrocatalytic Activity toward Ethanol Oxidation. *ACS Appl. Mater. Interfaces* **2013**, *5*, 11471−11478.

(25) Lee, K.; Kang, S. W.; Lee, S.-U.; Park, K.-H.; Lee, Y. W.; Han, S. W. One-Pot Synthesis of Monodisperse 5 nm Pd-Ni Nanoalloys for Electrocatalytic Ethanol Oxidation. *ACS Appl. Mater. Interface* **2012**, *4*, 4208−4214.

(26) Sun, H.; Jiao, X.; Wang, H.; Jiang, Z.; Chen, D. Solvothermal Preparation of Pd Nanostructures under Nitrogen and Air Atmospheres and Electrocatalytic Activities for the Oxidation of Methanol. *ACS Appl. Mater. Interfaces* **2011**, *3*, 2425−2430.

(27) Zhang, L.; Du, L.; Yu, X.; Tan, S.; Cai, X.; Yang, P.; Gu, Y.; Mai, W. Significantly Enhanced Photocatalytic Activities and Charge Separation Mechanism of Pd-Decorated ZnO−Graphene Oxide Nanocomposites. *ACS Appl. Mater. Interfaces* **2014**, *6*, 3623−3629.

(28) Kainz, Q. M.; Linhardt, R.; Grass, R. N.; Vilé, G.; Pérez-Ramírez, J.; Stark, W. J.; Reiser, O. Palladium Nanoparticles Supported on Magnetic Carbon-Coated Cobalt Nanobeads: Highly Active and Recyclable Catalysts for Alkene Hydrogenation. *Adv. Funct. Mater.* **2014**, *24*, 2020−2027.

(29) Yang, J.; Xie, Y.; Wang, R.; Jiang, B.; Tian, C.; Mu, G.; Yin, J.; Wang, B.; Fu, H. Synergistic Effect of Tungsten Carbide and Palladium on Graphene for Promoted Ethanol Electrooxidation. *ACS Appl. Mater. Interfaces* **2013**, *5*, 6571−6579.

(30) Sun, T.; Zhang, Z.; Xiao, J.; Chen, C.; Xiao, F.; Wang, S.; Liu, Y. Facile and Green Synthesis of Palladium Nanoparticles-Graphene-Carbon Nanotube Material with High Catalytic Activity. *Sci. Rep.* **2013**, *3*, 2527.

(31) Cornelio, B.; Rance, G. A.; Laronze-Cochard, M.; Fontana, A.; Sapib, J.; Khlobystov, A. N. Palladium Nanoparticles on Carbon Nanotubes as Catalysts of Cross-Coupling Reactions. *J. Mater. Chem. A* **2013**, *1*, 8737−8744.

(32) Cui, Z.; Gong, C.; Guo, C. X.; Li, C. M. Mo_2C/CNTs Supported Pd Nanoparticles for Highly Efficient Catalyst towards Formic Acid Electrooxidation. *J. Mater. Chem. A* **2013**, *1*, 1179−1184.

(33) Cai, Z.-x.; Liu, C-c.; Wu, G.-h.; Chen, X.-m.; Chen, X. Palladium Nanoparticles Deposit on Multi-Walled Carbon Nanotubes and Their Catalytic Applications for Electrooxidation of Ethanol and Glucose. *Electrochim. Acta* **2013**, *112*, 756−762.

(34) Mackiewicz, N.; Surendran, G.; Remita, H.; Keita, B.; Zhang, G. J.; Nadjo, L.; Hagege, A.; Doris, E.; Mioskowski, C. Supramolecular Self-Assembly of Amphiphiles on Carbon Nanotubes: A Versatile Strategy for the Construction of CNT/Metal Nanohybrids, Application to Electrocatalysis. *J. Am. Chem. Soc.* **2008**, *130*, 8110−8111.

(35) Carmo, M.; Paganin, V. A.; Rosolen, J. M.; Gonzlez, E. R. Alternative Supports for the Preparation of Catalysts for Low-Temperature Fuel Cells: The Use of Carbon Nanotubes. *J. Power Sources* **2005**, *142*, 169−176.

(36) Qu, L.; Dai, L. Substrate-Enhanced Electroless Deposition of Metal Nanoparticles on Carbon. *J. Am. Chem. Soc.* **2005**, *127*, 10806−10807.

(37) Quinn, B. M.; Dekker, C.; Lemay, S. G. Electrodeposition of Noble Metal Nanoparticles on Carbon Nanotubes. *J. Am. Chem. Soc.* **2005**, *127*, 6146−6147.

(38) Singh, R. N.; Singh, A.; Anindita, A. Electrocatalytic Activity of Binary and Ternary Composite Films of Pd, MWCNT, and Ni for Ethanol Electro-Oxidation in Alkaline Solutions. *Carbon* **2009**, *47*, 271−278.

(39) Hu, F. P.; Wang, Z.; Li, Y.; Li, C.; Zhang, X.; Shen, P. K. Improved Performance of Pd Electrocatalyst Supported on Ultrahigh Surface Area Hollow Carbon Spheres for Direct Alcohol Fuel Cells. *J. Power Sources* **2008**, *177*, 61−66.

(40) Tripkovic, A. V.; Popovic, K. D.; Lovic, J. D. The Influence of the Oxygen-Containing Species on the Electrooxidation of the C1-C4 Alcohols at Some Platinum Single Crystal Surfaces in Alkaline Solution. *Electrochim. Acta* **2001**, *46*, 3163−3173.

(41) Liang, Z. X.; Zhao, T. S.; Xu, J. B.; Zhu, L. D. Mechanism Study of the Ethanol Oxidation Reaction on Palladium in Alkaline Media. *Electrochim. Acta* **2009**, *54*, 2203−2208.

(42) Liu, H. P.; Ye, J. P.; Xu, C. W.; Jiang, S. P.; Tong, Y. X. Kinetics of Ethanol Electrooxidation at Pd Electrodeposited on Ti. *Electrochem. Commun.* **2007**, *9*, 2334−2339.

(43) Spendelow, J. S.; Wieckowski, A. Electrocatalysis of Oxygen Reduction and Small Alcohol Oxidation in Alkaline Media. *Phys. Chem. Chem. Phys.* **2007**, *9*, 2654−2675.

(44) Qin, Y. H.; Yang, H. H.; Zhang, X. S.; Li, P.; Zhou, X. G.; Niu, L.; Yuan, W. K. Electrophoretic Deposition of Network-Like Carbon Nanofibers as a Palladium Catalyst Support for Ethanol Oxidation in Alkaline Media. *Carbon* **2010**, *48*, 3323−3329.

(45) Hu, C.; Bai, Z.; Yang, L.; Lv, J.; Wang, K.; Guo, Y.; Cao, Y.; Zhou, J. Preparation of High Performance Pd Catalysts Supported on Untreated Multi-Walled Carbon Nanotubes for Formic Acid Oxidation. *Electrochim. Acta* **2010**, *55*, 6036−6041.

(46) Huang, H.; Wang, X. Pd Nanoparticles Supported on Low-Defect Graphene Sheets: For Use as High-Performance Electro-catalysts for Formic Acid and Methanol Oxidation. *J. Mater. Chem.* **2012**, *22*, 22533−22541.

(47) Guo, Q.; Liu, D.; Huang, J.; Hou, H.; You, T. A Composite Made from Palladium Nanoparticles and Carbon Nanofibers for Superior Electrocatalytic Oxidation of Formic Acid. *Microchim. Acta* **2014**, *181*, 797−803.

(48) Uhm, S.; Lee, H.-J.; Lee, J. Understanding Underlying Processes in Formic Acid Fuel Cells. *Phys. Chem. Chem. Phys.* **2009**, *11*, 9326−9336.

(49) Chen, Y.-X.; Heinen, M.; Jusys, Z.; Behm, R.-J. Bridge-Bonded Formate: Active Intermediate or Spectator Species in Formic Acid Oxidation on a Pt Film Electrode. *Langmuir* **2006**, *22*, 10399−10408.

(50) Wang, J.; Qin, Y.-L.; Liu, X.; Zhang, X.-B. In Situ Synthesis of Magnetically Recyclable Graphene-Supported Pd@Co Core-Shell Nanoparticles as Efficient Catalysts for Hydrolytic Dehydrogenation of Ammonia Borane. *J. Mater. Chem.* **2012**, *22*, 12468−12470.

(51) Capon, A.; Parsons, R. The Oxidation of Formic Acids on Noble Electrodes II, A Comparison of the Behavior of Pure Electrodes. *J. Electroanal. Chem.* **1973**, *44*, 239−254.

(52) Samjeske, G.; Miki, A.; Ye, S.; Osawa, M. Mechanistic Study of Electrocatalytic Oxidation of Formic Acid at Platinum in Acidic Solution by Time-Resolved Surface-Enhanced Infrared Absorption Spectroscopy. *J. Phys. Chem. B* **2006**, *110*, 16559−16566.

(53) Zhang, H.-X.; Wang, C.; Wang, J.-Y.; Zhai, J.-J.; Cai, W.-B. Carbon-Supported Pd-Pt Nanoalloy with Low Pt Content and Superior Catalysis for Formic Acid Electro-Oxidation. *J. Phys. Chem. C* **2010**, *114*, 6446−6451.

(54) Liu, Y.; Wang, L.-W.; Wang, G.; Deng, C.; Wu, B.; Gao, Y. High Active Carbon Supported PdAu Catalyst for Formic Acid Electro-oxidation and Study of the Kinetics. *J. Phys. Chem. C* **2010**, *114*, 21417−21422.

(55) Correia, A. N.; Mascaro, L. H.; Machado, S. A. S.; Avaca, L. A. Amorphous Palladium-Silicon Alloys for the Oxidation of Formic Acid and Formaldehyde. A Voltammetric Investigation. *J. Braz. Chem. Soc.* **1999**, *10*, 478−482.

(56) Gao, G.-Y.; Guo, D.-J.; Li, H.-L. Electrocatalytic Oxidation of Formaldehyde on Palladium Nanoparticles Supported on Multi-Walled Carbon Nanotubes. *J. Power Sources* **2006**, *162*, 1094−1098.

(57) Binder, H.; Köhling, I. A.; Kuhn, W.; Sandstede, G. Electrochemical Oxidation of Aldehydes, Formic Acid, and Carbon Monoxide at Tungsten Carbide Electrodes in 2 *N* Sulfuric Acid. *Angew. Chem., Int. Ed.* **1969**, *8*, 757−758.
(58) Niu, F.; Yi, Q. A Novel Nanoporous Palladium Catalyst for Formaldehyde Electro-Oxidation in Alkaline Media. *Rare Met.* **2011**, *30*, 102−105.
(59) Wan, Q.; Wang, X.; Yu, F.; Wang, X.; Yang, N. Effects of Capacitance and Resistance of MWNT-Film Coated Electrodes on Voltammetric Detection of Acetaminophen. *J. Appl. Electrochem.* **2009**, *39*, 1145−1151.
(60) Wan, Q.; Wang, X.; Yu, F.; Wang, X.; Yang, N. Poly(Taurine)/MWNTs-Modified Glassy Carbon Electrodes for the Detection of Acetaminophen in Drugs. *J. Appl. Electrochem.* **2009**, *39*, 785−790.
(61) Ellis, A. V.; Vjayamohanan, K.; Goswaimi, R.; Chakrapani, N.; Ramanathan, L. S.; Ajayan, P. M.; Ramanath, G. Hydrophobic Anchoring of Monolayer-Protected Gold Nanoclusters to Carbon Nanotubes. *Nano Lett.* **2003**, *3*, 279−282.
(62) Burda, C.; Chen, X. B.; Narayanan, R. Chemistry and Properties of Nanocrystals of Different Shapes. *Chem. Rev.* **2005**, *105*, 1025−1102.